COMPDYN 2025
10th ECCOMAS Thematic Conference on
Computational Methods in Structural Dynamics and Earthquake Engineering
M. Papadrakakis, M. Fragiadakis (eds.)
Rhodes Island, Greece, 15-18 June 2025

A NEW GLOBAL DATABASE OF SEISMIC VULNERABILITY MODELS FOR IMPROVED REGIONAL RISK ASSESSMENTS

Karim Aljawhari[1,2], Al Mouayed Bellah Nafeh[1], and Vitor Silva[1]

[1] Global Earthquake Model (GEM) Foundation
Via Adolfo Ferrata 1, Pavia, Italy

{karim.aljawhari,mouayed.nafeh,vitor.silva}@globalquakemodel.org

Abstract

This study introduces a comprehensive global vulnerability database designed to enhance regional seismic risk assessments. It addresses the limitations of existing databases, which often rely on oversimplified models that fail to capture story-level engineering demand parameters and some seismic response patterns. Covering more than 1,400 building classes, the database incorporates an advanced numerical modelling approach, utilizing stick-and-mass multi-degree-of-freedom oscillators. Key contributions include: 1) a suite of updated vulnerability functions for structural damage across building types; 2) a set of region-specific story-loss functions, which use story demands like drifts and floor accelerations to produce more robust estimates of losses due to non-structural damage; and 3) a dataset of vulnerability functions for losses in building contents. To demonstrate the value of the new database, we perform a comparison between the new vulnerability functions and those in the original version of the database, which were derived from simplified single-degree-of-freedom models.

Keywords: Earthquake Engineering, Seismic Vulnerability Assessment, Multi-Degree of Freedom, Story Loss Functions, Regional Risk Assessment

1. INTRODUCTION

Over the past century, earthquakes have caused nearly one million fatalities and one trillion USD in economic losses, primarily due to the poor seismic performance of vulnerable buildings. This highlights the importance of reliable performance assessments for building to understand seismic risk drivers and aid decision-making for mitigation [1]. These assessments must account for damage in structural components, non-structural components and building contents, which represent over 50% of the buildings' value across the globe [2].

The Global Earthquake Model (GEM) Foundation's first database of fragility and vulnerability functions, introduced by Martins and Silva [3], included nearly 500 building classes modelled as simplified single-degree-of-freedom (SDOF) systems. While useful for regional analysis, these models cannot capture some complex behaviors such as higher-mode effects or story-level demands like peak story drift (PSD) and peak floor acceleration (PFA), limiting their reliability for non-structural and contents loss estimation.

To address these gaps, detailed component-based multi-degree-of-freedom (MDOF) models are often adopted to improve accuracy, but they are computationally expensive and impractical at regional scales. On the other hand, intermediate models, such as stick-and-mass MDOF systems, offer a promising balance, enabling the incorporation of higher-mode effects. They further capture story-level seismic demands (e.g., PSD and PFA) with greater computational efficiency [4–6], which can be used with story-loss functions (SLFs) [7] to produce refined loss estimates at story level, especially for non-structural components [8].

This study expands Martins and Silva's database [9] from 500 to over 1,400 building classes and replaces SDOF models with the more robust stick-and-mass MDOF oscillators. It introduces new fragility and vulnerability functions that provide enhanced damage and loss estimates for structural components and building contents, in addition to a set of vulnerability functions derived using region-specific SLFs to quantify losses in drift-sensitive and acceleration sensitive non-structural components. The new database is compared against the original version, revealing major differences that highlight the role of robust vulnerability modelling in robust risk management.

2. GLOBAL VULNERABILITY DATABASE

2.1. Global Building Class Coverage

The updated vulnerability database expands building classes from 500 to over 1,400, covering a wide range of structural attributes and geometric characteristics that affect seismic performance. Buildings are categorized based on key factors including primary construction materials, lateral load-resisting systems, seismic code levels, and ductility levels. The database also incorporates region-specific attributes influencing non-structural performance, such as non-structural component anchorage, dominant inelastic mechanisms, and floor type. Additional classification factors include height (number of stories) and occupancy (residential, commercial, industrial), which impact the type and quantity of non-structural components and contents. Figure 1 shows the distribution of these attributes across building classes in the database. Further details are available in Yepes-Estrada et al. [10].

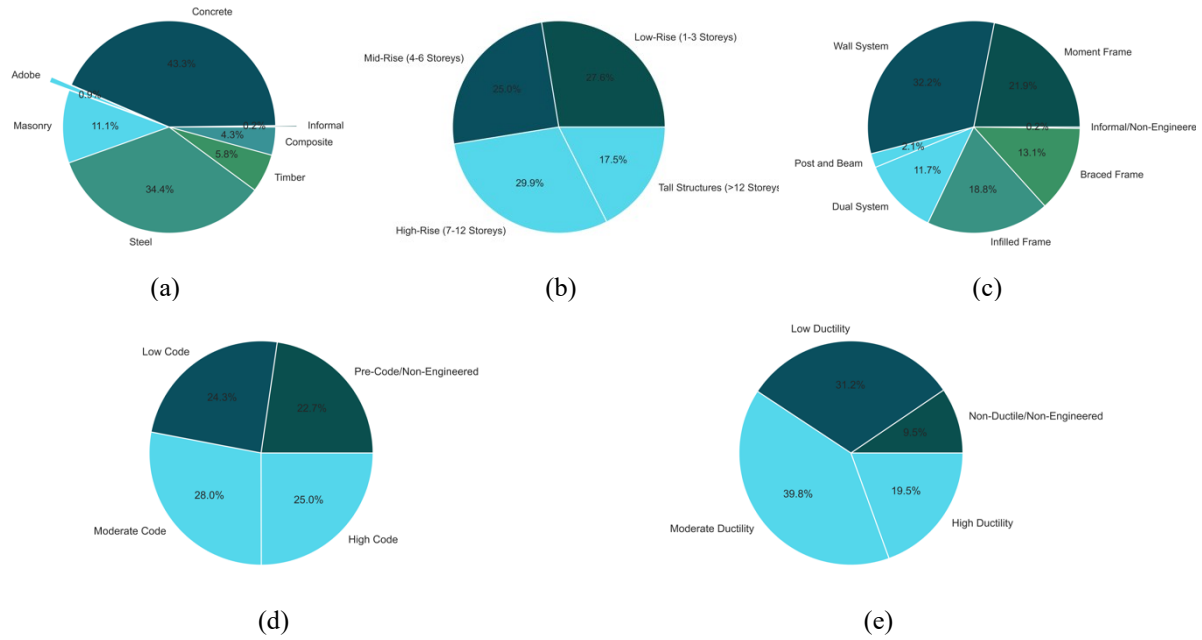


Figure 1: Distribution of building classes by (a) material, (b) number of stories, (c) lateral load-resisting system, (d) code level, and (e) ductility level.

2.2. Numerical Modelling

The original vulnerability database by Martins and Silva [3] used simplified SDOF models. The updated version adopts stick-and-mass MDOF models to capture story-level demands such as PSD and PFA, along with higher-mode effects and demand concentrations. In the new models, masses are concentrated at each floor and connected by nonlinear springs that define the shear force-drift behaviour (Figure 2). These models assume a shear-dominated response and do not account for torsional modes, but still offer high reliability and computational efficiency for regional seismic risk assessments [11,12]. The MDOF systems are implemented in OpenSeesPy [13], using the "Pinching4" material to define shear force-drift relationships with bilinear, tri-linear, or quadrilinear backbone curves, depending on the type of building nonlinear response.

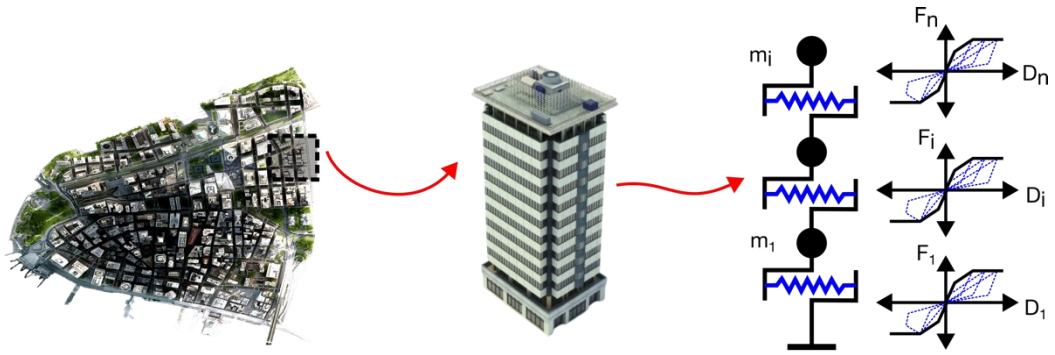


Figure 2: MDOF idealization of regional building stock

The stick-and-mass MDOF models are derived on the basis of the SDOF capacity curves in the original database of Martins and Silva, where the capacity is expressed as a relationship between spectral acceleration (*SA*) and displacement (*SD*). The derivation relies on the approach proposed by Lu et al. [12], which was originally developed to calibrate MDOF stick models from the HAZUS capacity-curve database [14]. This method uses the principles of structural dynamics to convert the capacity curve to the pushover curve of the corresponding MDOF system, which describes the relationship between roof displacement and base shear. This relationship is then proportioned for individual stories based on the first-mode shape. More details can be found in Lu et al. [12]. An example is shown in Figure 3 for the calibration.

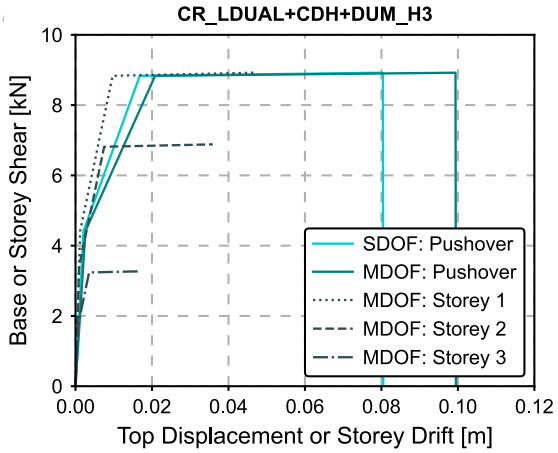


Figure 3: SDPF and MDOF pushover curves, with story shear vs. drift for a 3-storey reinforced concrete dual system with high code and medium ductility

The numerical modelling procedure described above is further facilitated with the development of the Vulnerability Modelers Toolkit (oq-vmtk). The oq-vmtk is an open-source library designed for comprehensive seismic vulnerability assessment built with OpenSeesPy. It enables researchers, engineers and earthquake catastrophe modelers to: 1) develop single- and multi-degree-of-freedom models; 2) conduct nonlinear time-history analyses; 3) derive both fragility and vulnerability functions. The oq-vmtk supports a range of analysis types, like modal, gravity, nonlinear static (i.e., pushover) and dynamic time-history analyses (i.e., cloud analysis). The toolkit features a visualization library for seismic demand profiles, fragility curves and vulnerability functions further assisting developers in efficiently debugging their numerical models. The toolkit is available on https://github.com/GEMScienceTools/oq-vmtk.

2.3. Loss Modelling

2.3.1. Structural Losses

To derive structural losses, fragility functions for structural damage for each building class, quantifying the probability of exceeding various damage states (DSs) across a range of intensity measures (IMs) were first calculated. Four global DSs are considered: slight, moderate, extensive, and complete. These states are identified through structural analysis when predefined thresholds of an engineering demand parameter (EDP) are reached, with maximum interstorey drift ratio or θ_{max} chosen due to its strong correlation with global structural damage.

In the original database by Martins and Silva [3], DS thresholds for structural damage in SDOF oscillators were expressed in terms of spectral displacement. In this study, these thresholds are converted to θ_{max} for MDOF systems, as detailed in Table 1, following structural dynamic principles. The yield (SD_y) and ultimate (SD_u) spectral displacement are acquired from the capacity curves in the original vulnerability database. hi is the height of the "i-th" story and Γ_1 is the first-mode modal transformation factor. To convert each DS to the corresponding loss, damage-to-loss ratios are used [15,16], which represent the repair cost of the DS, normalized by the building's structural replacement cost. These are also reported in Table 1.

Table 1: MDOF damage state thresholds for the four damage states

Damage State	Maximum Interstorey Drift Ratio Threshold	Mean Damage-to-Loss Ratio
Slight	$\theta_{max,DS} = max_{i=1,..n_s}\left[\frac{\Gamma_1(\phi_{1,i} - \phi_{1,i-1})SD_y}{h_i}\right]$	5%
Moderate	$\theta_{max,DS} = max_{i=1,..n_s}\left[\frac{\Gamma_1(\phi_{1,i} - \phi_{1,i-1})(0.67SD_y + 0.33SD_u)}{h_i}\right]$	20%
Extensive	$\theta_{max,DS} = max_{i=1,..n_s}\left[\frac{\Gamma_1(\phi_{1,i} - \phi_{1,i-1})(0.33SD_y + 0.67SD_u)}{h_i}\right]$	60%
Complete	$\theta_{max,DS} = max_{i=1,..n_s}\left[\frac{\Gamma_1(\phi_{1,i} - \phi_{1,i-1})SD_u}{h_i}\right]$	100%

Based on the above information, fragility functions for structural damage are derived via the cloud analysis approach [17], which subjects the structure to a set of unscaled ground-motion records. A set of 700 records is used here, acquired from different strong-motion databases [18–20]. Probabilistic seismic demand models are then fitted to the results of cloud analysis to characterize the relationship between IM and EDP using a power-law function (Equation 1). Fragility functions are finally derived as lognormal cumulative distribution functions, with the following statistical parameters (see Equation 2):

- μ_{DS}: median
- $\beta_{TOTAL} = \sqrt{\beta_{RTR}^2 + \beta_{MOD}^2}$: total dispersion accounting for the record-to-record variability β_{RTR}^2 and the modelling uncertainty β_{MOD}^2 (set to 0.30)

Subsequently, structural vulnerability functions representing the normalized economic loss due to structural damage across varying IM values, $E(LR_S|IM)$, are derived for all building classes. These functions are derived by combining the fragility functions with appropriate damage-to-loss ratios (Table 1) via Equation 3. To account for the uncertainty in $E(LR_S|IM)$, the approach proposed by Silva [21] is applied. This method quantifies the influence of record-to-record variability on seismic loss predictions across different structural systems. The standard deviation in the loss ratio given IM, denoted as $\sigma_{LR|IM}$ is estimated using a semioval curve approximation, as expressed in Equation 4.

$$EDP = \alpha IM^{\beta} \quad \text{Equation 1}$$

$$P(DS \geq DS_i|IM) = \Phi\left(\frac{lnIM/\mu_{DSi}}{\beta_{TOTAL}}\right) \quad \text{Equation 2}$$

$$E(LR_S|IM) = \sum_{i=1}^{nDS} P(DS = DS_i|IM) LR_{DSi} \quad \text{Equation 3}$$

$$\sigma_{LR_S|IM} = \sqrt{E(LR_S|IM)\,(-0.7 - 2\,E(LR_S|IM) + \sqrt{6.8\,E(LR_S|IM) + 0.5})} \quad \text{Equation 4}$$

It should be noted that the fragility and vulnerability functions are derived for different IM types, including Peak Ground Acceleration (PGA), 5%-damped Spectral Acceleration at 0.3, 0.6 and 1.0s (SA(0.3s), SA(0.6s), SA(1.0s)), average spectral acceleration at a period range of 0.1-1.0s (AvgSA).

2.3.2. Building Contents Losses

Building contents refer to the non-structural items inside a building that are not part of its structural or architectural systems and do not contribute to its functionality. These include furniture, equipment, appliances, and other movable objects that can be damaged or displaced during an earthquake. Contents fragility and vulnerability derivation is similar to structural components, however, there are key distinctions, particularly regarding the way damage states are considered. For instance, building content damage is classified as either completely damaged or non-damaged because contents are likely to be replaced under any level of damage (e.g., if a television breaks, it is completely unusable). Moreover, the EDP used to characterize content damage is the maximum PFA. Therefore, PFA is used as EDP instead of MIDR in Equation 1.

The PFA thresholds defining whether building contents are damaged depend on the ductility of the structure (e.g., low, high) and the occupancy type (e.g., residential, commercial, or industrial), and they are obtained from the HAZUS Technical Manual [14]. Content fragility functions are eventually derived as lognormal cumulative distributions, with median and dispersion parameters (μ_{DS} and β_{TOTAL}) like those used for structural components. To convert fragility into vulnerability functions, $E(LR_C|IM)$, a damage-to-loss model is used. Given that the DSs of building contents are binary (either damaged or undamaged), the damage-to-loss model has a unity value (complete loss) if contents are damaged and zero if contents are undamaged.

2.3.3. Nonstructural Losses

Nonstructural components refer to the various parts and elements of a building or structure that do not contribute to its primary load-bearing function but serve functional, aesthetic, and operational purposes. This includes architectural features and electrical/mechanical fixtures such as:

- Interior finishes**:** flooring, ceilings, partitions, and wall finishes.
- Mechanical, electrical, and plumbing systems (MEP)**:** HVAC (heating, ventilation, and air conditioning), electrical wiring, elevators, lighting, water supply, sewage systems, and fire protection systems.
- Windows and doors
- Exterior finishes: these include cladding and exterior facades.
- Internal and external partitions.

Unlike structural fragility and vulnerability, non-structural vulnerability functions defining the expected loss ratio, given the intensity measure level, $E(LR_{NS}|IM)$, are not derived from the global DSs. Instead, they are created by aggregating losses sustained by individual stories via SLFs that express these losses as a function of the EDP attained at each story or floor, such as PSD and PFA (see Figure **4**). This method provides more precise loss estimates, which is crucial since non-structural components often drive economic losses, particularly at lower IM levels. To this end, a comprehensive data collection is carried out to construct region-specific story loss functions, which include:

- Review of normalized nonstructural component quantities (i.e., per m^2 floor area) found typically in distinct building and occupancy (i.e., residential, commercial, industrial) classes
- Review of regional repair costs associated with damage to nonstructural components
- Resolving missing data with information from complete databases such as FEMA P-58 [22] and additional literature [23,24]
- Derivation of story loss functions using oq-vmtk for drift- and acceleration-sensitive components

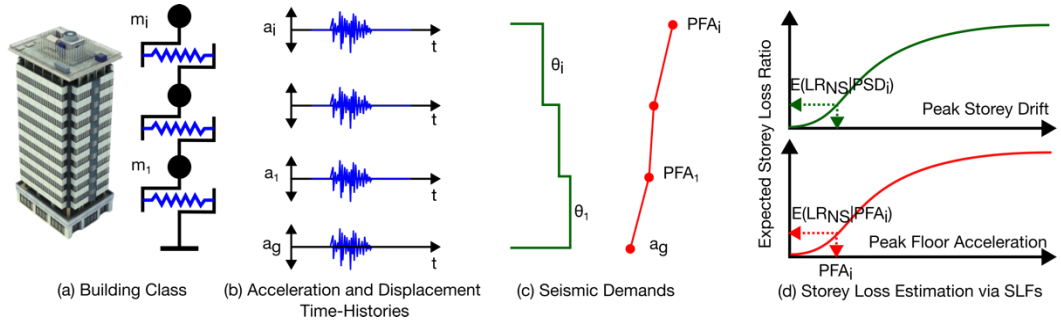


Figure 4: Estimation of story-based nonstructural losses coupling seismic demands distribution for MDOF idealizations and storey loss functions

Once the building is analyzed via NLTHA, the total non-structural loss ratio associated with each ground motion ground motion can be computed using the relevant EDPs and SLFs and then aggregated across all stories and floors. The non-structural vulnerability function, $E[LR_{NS}|IM]$, is finally characterized by fitting a Weibull regression model using the method described in [25].

3. RESULTS AND DISCUSSION

This section provides key comparisons between the new and original vulnerability databases in terms of fragility and vulnerability functions. Figure 5(a-c) compares the μ_{DS} values of structural fragility functions across different building height ranges. The horizontal axis has the values from the new database, while the vertical axis shows the values of the original database. For one-story buildings (Figure 5(a)), which have a SDOF in both databases, the μ_{DS} values are identical. Figure 5(b) depicts buildings up to 8 stories, which show slight deviations in μ_{DS} due to the updated modelling strategy, which accounts for higher-mode effects. The average difference is within 18%, so it is not anticipated to significantly affect regional risk analyses. Figure 5(c) reports the μ_{DS} for building classes ranging from 8 to 20 stories. The average difference exceeds 40% compared to the original database, which is attributed to the lack of higher-mode

effects in SDOF models although they can cause larger deformation. Hence, the old models may significantly underestimate seismic losses.

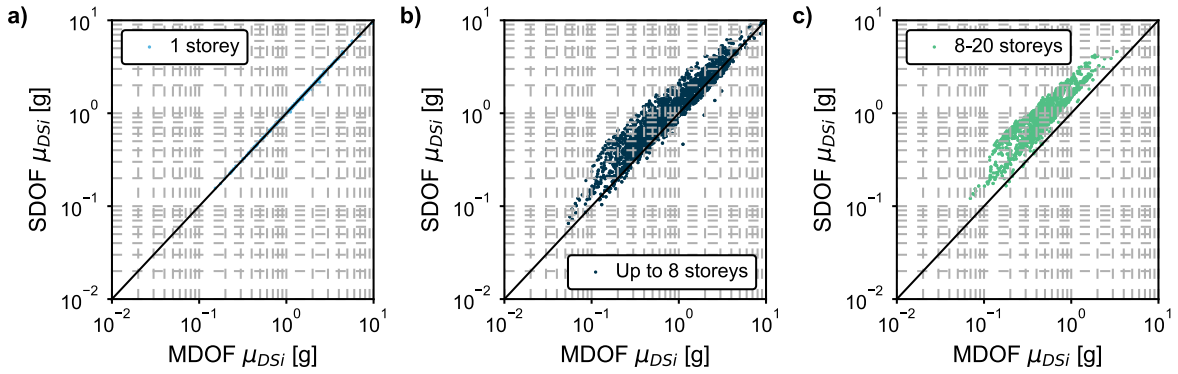


Figure 5. The new vs. original databases in terms of $\boldsymbol{\mu_{DS}}$ for structural building-level fragility: a) one-story; b) up to 8 stories; and c) 8-20 stories

The above trends are confirmed in Figure 6, which compares structural vulnerability functions for mid-rise and high-rise reinforced concrete dual systems. For the mid-rise building (5 stories) in Figure 6(a), the functions are not very different, whereas Figure 6(b) demonstrates that the losses in the high-rise (35 stories) from the MDOF modelling strategy to 2.5 higher than those calculated through the SDOF vulnerability function.

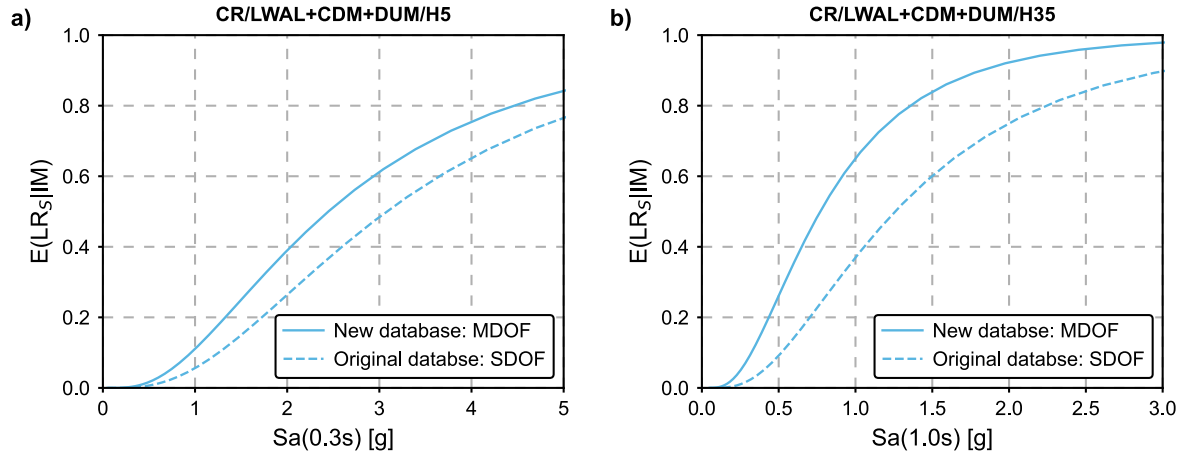


Figure 6. The new vs. original databases in terms of structural vulnerability for reinforced concrete dual system with medium code level and ductility class: (a) 5 stories; and (b) 35 stories

Figure 7 presents a further comparison but considering non-structural vulnerability functions for two residential building classes. These are a high code 5-storey reinforced concrete moment frame with high ductility (Figure 7(a)), and a moderate code 2-storey steel moment frame with high ductility (Figure 7(b)). The $E(LR_{NS}|IM)$ values are significantly lower considering the new MDOF models, which exceeds 35% at some IM levels. This can be explained by the fact that the new non-structural vulnerability functions are based on SLFs that capture story demands, allowing for more refined loss predictions. The original SDOF models, on the other hand, provide a single drift or acceleration values, which can overestimate losses.

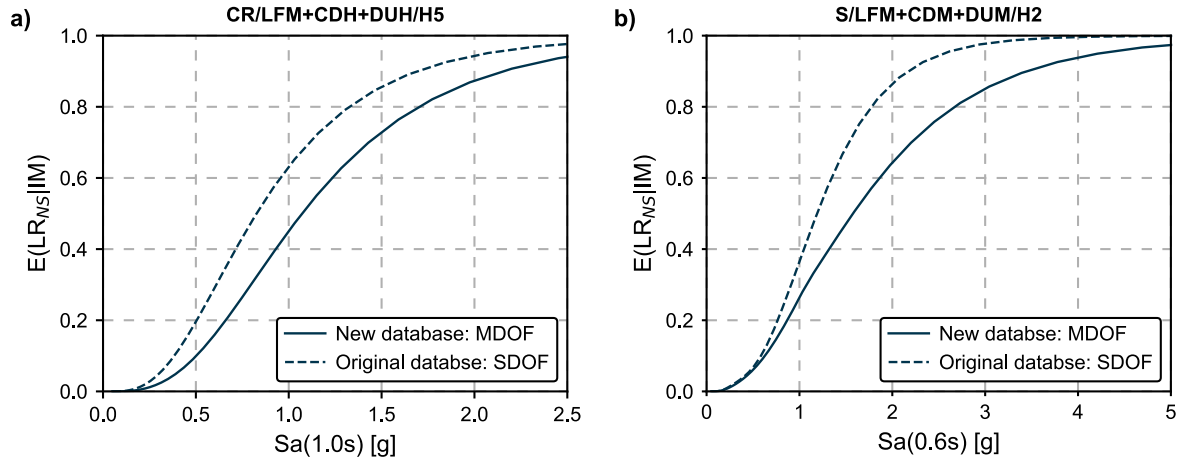


Figure 7. The new vs. original databases in terms of non-structural vulnerability functions for (a) residential 5-story reinforced concrete moment frame with high code and ductility, and (b) residential 2-story steel moment frame with medium code and ductility.

4. CONCLUSION

This study presented a comprehensive global seismic vulnerability database that delivers detailed fragility and vulnerability functions tailored regional risk assessments. This database adopts an advanced and effective numerical modeling approach featuring stick-and-mass MDOF oscillators to provide reliable seismic response simulations across a broad range of building classes. Leveraging the early version of the database by Martins and Silva[9], the updated global vulnerability database enhances risk assessments through these innovations:

- A broad inventory of over 1,400 building classes, encompassing diverse construction materials, lateral load-resisting systems, code compliance levels, ductility characteristics, and building heights.
- A refined numerical modeling approach that upgrades the simplified SDOF systems from the original dataset to stick-and-mass MDOF oscillators. This allows for explicitly estimating story-level demands and captures complex seismic behaviors such as soft-story and higher-mode effects, improving damage and loss characterization.
- A new set of building-level fragility and vulnerability functions for structural damage and loss, derived using the new MDOF oscillators.
- A parallel set of fragility and vulnerability functions for building contents.
- A detailed dataset of region-specific SLFs for losses in non-structural components at the story level. Corresponding vulnerability functions for non-structural losses over a range of IM levels were also generated.
- The oq-vmtk – an open-source automated vulnerability assessment toolkit that transforms SDOF models into MDOF stick-and-mass oscillators, performs a variety of seismic analyses, and generates all associated fragility and vulnerability outputs.

REFERENCES

1. Aljawhari K, Gentile R, Galasso C. Beyond Direct Economic Losses: An Integrated Approach to Seismic Retrofit Considering Sustainability and Indirect Losses. *Earthquake Engineering & Structural Dynamics* 2025. DOI: 10.1002/eqe.4324.

2. Yepes-Estrada C, Calderon A, Costa C, Crowley H, Dabbeek J, Hoyos MC, *et al.* Global building exposure model for earthquake risk assessment. *Earthquake Spectra* 2023; **39**(4): 2212–2235. DOI: 10.1177/87552930231194048.
3. Martins L, Silva V. Development of a fragility and vulnerability model for global seismic risk analyses. *Bulletin of Earthquake Engineering* 2021; **19**(15): 6719–6745. DOI: 10.1007/s10518-020-00885-1.
4. Jamšek A, Dolšek M. Seismic analysis of older and contemporary reinforced concrete frames with the improved fish-bone model. *Engineering Structures* 2020; **212**: 110514. DOI: 10.1016/j.engstruct.2020.110514.
5. Khaloo AR, Khosravi H. Modified fish-bone model: A simplified MDOF model for simulation of seismic responses of moment resisting frames. *Soil Dynamics and Earthquake Engineering* 2013; **55**: 195–210. DOI: 10.1016/j.soildyn.2013.09.013.
6. Gaetani d'Aragona M, Polese M, Di Ludovico M, Prota A. The use of Stick-IT model for the prediction of direct economic losses. *Earthquake Engineering & Structural Dynamics* 2021; **50**(7): 1884–1907. DOI: 10.1002/eqe.3429.
7. Ramirez C, Miranda E. *Building-specific loss estimation methods and tools for simplified performance-based earthquake engineering*. Stanford: 2009.
8. O'Reilly GJ, Shahnazaryan D. On the utility of story loss functions for regional seismic vulnerability modeling and risk assessment. *Earthquake Spectra* 2024; **40**(3): 1933–1955. DOI: 10.1177/87552930241245940.
9. Martins L, Silva V. Development of a fragility and vulnerability model for global seismic risk analyses. *Bulletin of Earthquake Engineering* 2021; **19**(15): 6719–6745. DOI: 10.1007/s10518-020-00885-1.
10. Yepes-Estrada C, Calderon A, Costa C, Crowley H, Dabbeek J, Hoyos MC, *et al.* Global building exposure model for earthquake risk assessment. *Earthquake Spectra* 2023; **39**(4): 2212–2235. DOI: 10.1177/87552930231194048.
11. Gaetani d'Aragona M, Polese M, Di Ludovico M, Prota A. Large scale loss assessment using stick-it model: A comparison with actual cost data. *Soil Dynamics and Earthquake Engineering* 2022; **160**: 107363. DOI: 10.1016/j.soildyn.2022.107363.
12. Lu X, McKenna F, Cheng Q, Xu Z, Zeng X, Mahin SA. An open-source framework for regional earthquake loss estimation using the city-scale nonlinear time history analysis. *Earthquake Spectra* 2020; **36**(2): 806–831. DOI: 10.1177/8755293019891724.
13. Zhu M, McKenna F, Scott MH. OpenSeesPy: Python library for the OpenSees finite element framework. *SoftwareX* 2018; **7**: 6–11. DOI: 10.1016/j.softx.2017.10.009.
14. Federal Emergency Management Agency. *Hazus ®-MH 2.1 Technical Manual. Washington D.C.: 2012*. Washington, DC.: 2012.
15. Aljawhari K, Gentile R, Galasso C. Earthquake-induced environmental impacts for residential Italian buildings: Consequence models and risk assessment. *Journal of Building Engineering* 2024; **84**. DOI: 10.1016/j.jobe.2023.108149.
16. Aljawhari K, Gentile R, Galasso C. Simulation-based consequence models of seismic direct loss and repair time for archetype reinforced concrete frames. *Soil Dynamics and Earthquake Engineering* 2023; **172**: 107979. DOI: 10.1016/j.soildyn.2023.107979.
17. Jalayer F, Ebrahimian H, Miano A, Manfredi G, Sezen H. Analytical fragility assessment using unscaled ground motion records. *Earthquake Engineering & Structural Dynamics* 2017; **46**(15): 2639–2663. DOI: 10.1002/eqe.2922.
18. Luzi L., Lanzano G., Felicetta C., D'Amico M. C., Russo E., Sgobba S., *et al. Engineering Strong Motion Database (ESM) (Version 2.0)*. 2020.

19. Bozorgnia Y, Abrahamson NA, Atik L Al, Ancheta TD, Atkinson GM, Baker JW, *et al.* NGA-West2 Research Project. *Earthquake Spectra* 2014; **30**(3): 973–987. DOI: 10.1193/072113EQS209M.
20. National Research Institute for Earth Science and Disaster Resilience. *NIED K-NET, KiK-net*. 2019.
21. Silva V. Uncertainty and Correlation in Seismic Vulnerability Functions of Building Classes. *Earthquake Spectra* 2019; **35**(4): 1515–1539. DOI: 10.1193/013018EQS031M.
22. Federal Emergency Management Agency (FEMA). *FEMA P-58-1, Seismic Performance Assessment of Buildings, Volume 1 – Methodology*. Washington, DC.: 2018.
23. Papadopoulos AN, Vamvatsikos D, Kazantzi AK. Development and Application of FEMA P-58 Compatible Story Loss Functions. *Earthquake Spectra* 2019; **35**(1): 95–112. DOI: 10.1193/102417EQS222M.
24. Silva A, Castro JM, Monteiro R. A rational approach to the conversion of FEMA P-58 seismic repair costs to Europe. *Earthquake Spectra* 2020; **36**(3): 1607–1618. DOI: 10.1177/8755293019899964.
25. Shahnazaryan D, O'Reilly GJ, Monteiro R. Story loss functions for seismic design and assessment: Development of tools and application. *Earthquake Spectra* 2021; **37**(4): 2813–2839. DOI: 10.1177/87552930211023523.